Variational Monte Carlo calculation of the nematic state of the two-dimensional electron gas in a magnetic field

Quoc M. Doan[1] and Efstratios Manousakis[1,2]
[1]*Department of Physics and MARTECH, Florida State University, Tallahassee, Florida 32306-4350, USA*
[2]*Department of Physics, University of Athens, Penipistimiopolis, Zografos, 157 84 Athens, Greece*
(Received 16 May 2008; revised manuscript received 22 July 2008; published 18 August 2008)

We use a Jastrow-Slater wave function with an elliptical Fermi sea to describe the nematic state of the two-dimensional electron gas in a magnetic field and the Monte Carlo method to calculate a variational energy upper bound. These energy upper bounds are compared with other upper bounds describing stripe-ordered ground states, which are obtained from optimized Hartree-Fock calculations, and with those which correspond to an isotropic ground state. Our findings support the conclusions drawn in our previous study, where the Fermi-hypernetted chain approximation was used instead of the Monte Carlo method. Namely, the nematic state becomes energetically favorable relative to the stripe-ordered Wigner crystal phase for the second excited Landau level and below a critical value of the layer "thickness" parameter, which is very close to its value in the actual materials.

DOI: 10.1103/PhysRevB.78.075314 PACS number(s): 73.43.Cd, 73.43.Lp

I. INTRODUCTION

The measurements of Lilly *et al.*[1] and Du *et al.*[2] reveal strong anisotropic transport properties of the two-dimensional electron gas (2DEG) for the half-filled Landau-level (LL) system for high LLs and at very low temperature. The anisotropic behavior in the transport properties is consistent with stripe and bubble charge-density-wave phases, which were predicted early on in Refs. 3–5 by means of Hartree-Fock (HF) calculations of the 2DEG and were confirmed more recently by numerical studies of systems with up to 12 electrons.[6,7] However, Fradkin *et al.*[8] have challenged this interpretation and suggested that the anisotropic transport might be due to a possible nematic phase of the 2DEG in a magnetic field. This idea finds support in the good comparison between the results of the temperature dependence of the anisotropy of the resistivity obtained by means of a Monte Carlo (MC) simulation of the nematic phase[9] with that which has been experimentally observed. In addition, the idea is supported by the experiments of Cooper *et al.*[10] where an in-plane magnetic field was applied in the 2DEG and the results of the experiment were interpreted on the basis of the presence of a nematic state; further support of the idea is provided by the fact that the theoretically estimated transition temperature from an isotropic to nematic phase[11] is of similar magnitude as the experimentally determined temperature at which the onset of the anisotropic transport occurs.

Rather recently, we have presented[12] a variational calculation of the nematic state as ground state of the half-filled LL system in a magnetic field based on an ansatz ground-state wave function proposed by Oganesyan *et al.*,[13] which is of the Jastrow-Slater form and is given by the following expression:

$$\Psi(\vec{r}_1,\vec{r}_2,\ldots,\vec{r}_N) = \hat{P}_0 \prod_{j<k}^{N} (z_j - z_k)^2 e^{-\Sigma_{k=1}^{N}|z_k|^2/4} \times \det|\varphi_{\vec{k}}(\vec{r}_i)|, \quad (1)$$

where $\hat{P}_0$ is the projection operator onto the lowest LL (LLL) and $\phi_{\vec{k}}(\vec{r}_i)$ are 2D plane-wave states. Here, $z_j = x_j + iy_j$ is the complex 2D coordinate of the j electron. This wave function is a Jastrow correlated Slater determinant with Jastrow part similar to the Laughlin state.[14] This ground-state wave function has the same form as the form proposed by Rezayi and Read;[15] however, the single-particle momenta form an elliptical Fermi sea as opposed to the circular Fermi sea. There is a broken-symmetry parameter, which is the ratio $\alpha = k_1/k_2$ of the semimajor k_1 and semiminor k_2 axes of the elliptical Fermi sea. Using this wave function to describe the nematic state, we had carried out a variational study of the half-filled system using the so-called Fermi-hypernetted-chain (FHNC) approximation.[12]

The results of the above mentioned variational calculation indicate that there is a certain value of the parameter λ (λ is proportional to the 2DEG layer thickness[16]) below which the nematic state is energetically favorable as compared to the isotropic and the stripe-ordered ground states for the second excited LL. It is interesting to note that this critical value of λ is very close to the value of λ, which can be estimated based on the actual experimental conditions which are applicable for the case of the data by Lilly *et al.*[1] and by Du *et al.*[2] However, one of the weak points of the above described variational study is the fact that the FHNC approximation is plagued by an unknown-size error and the results cannot be improved in a controlled manner.[17] Therefore, there is a need to check the validity of these results and conclusions using the variational MC method and this task is undertaken in the present work.

There is a different variational approach to the problem of a broken rotational state of the half-filled LL introduced by Ciftja and Wexler.[18] They have used the FHNC approximation to study a broken rotational state of the half-filled LL, where the symmetry-breaking parameter was introduced in the correlation part of the wave function as $(z_i - z_j)^2 \rightarrow (z_i - z_j - \alpha)(z_i - z_j + \alpha)$, and they used the standard single-particle determinant with a circular Fermi sea.

In this paper and in the work of Ref. 12, we considered the unprojected wave function of the nematic state. The ad-

vantage of this simplified version is that it has a Jastrow form with a Slater determinant so it can be applied directly with FHNC and it allows us to study large-size systems using the variational MC method. The paper is organized as follows: In Sec. II we discuss the formulation and the procedure. In Sec. III we present the results and we compare them with those obtained for the case of a stripe-ordered and the isotropic states. In Sec. IV we summarize the conclusions of the present calculation.

II. METHOD

We have adopted the toroidal geometry of a square with periodic boundary conditions. This geometry has the advantage of naturally adapting to the nematic and isotropic state wave function. There are several steps in applying the MC approach for this problem. First, as part of the wave function of nematic state, we construct a Slater determinant of plane waves characterized by momentum vectors, which lie inside an elliptical Fermi sea. Second, since the pseudopotential is $\ln(r)$, which is a long-range interaction, we need to to take into account all periodic image charge interactions. One of the methods to do this is the Ewald summation technique. In Appendix A1, we describe the Ewald summation technique for the case of toroidal boundary conditions and the $\ln(r)$ interaction. In the present section, we will discuss our implementation of the MC to study the nematic state.

Given a value of α there are definite values of the number of particles N, which correspond to a closed shell. These definite values of N are calculated as follows. The occupied states characterized by k_x, k_y must satisfy the following condition:

$$\left(\frac{k_x}{k_1}\right)^2 + \left(\frac{k_y}{k_2}\right)^2 \leq 1, \tag{2}$$

where k_1 and k_2 are the major and minor axes of the Fermi sea and are given by

$$k_1 = \sqrt{\frac{4\pi\rho}{\alpha}}, \tag{3}$$

$$k_2 = \sqrt{4\pi\rho\alpha}, \tag{4}$$

where ρ is the uniform particle density of the system. For a finite system of size $L \times L$, $k_x = n_x \Delta k$, and $k_y = n_y \Delta k$ where $\Delta k = 2\pi/L$ and $n_x, n_y \in Z$. So one can deduce the conditions for n_x, n_y, such that

$$\frac{\pi}{N}\left(\alpha n_x^2 + \frac{n_y^2}{\alpha}\right) \leq 1. \tag{5}$$

For a value of N to be acceptable, the number of states, i.e., the number of pairs (n_x, n_y) satisfying the above inequality should be equal to N. For example, for $\alpha=1$, N can be 1,5,9,13,21,25,29,37,45,…; for $\alpha=2$, they can be 1,3,7,11,15,17,21,….

In Fig. 1, we present two examples of closed shell, which correspond to $\alpha=2$ and 4 for $N=89$. Notice that with anisotropy parameter $\alpha = k_x/k_y > 1$, the occupied states (i.e, those satisfying Eq. (5)) are anisotropically distributed along the preferred k_x axis. In our MC calculation, we will use these cases as well as larger size systems up to 145 particles.

We follow the metropolis MC scheme for sampling the wave function where the ratio needed between the new and the old wave function is

$$\left|\frac{\psi(\vec{r}_{\text{new}})}{\psi_{(\vec{r}_{\text{old}})}}\right|^2 = \exp(u(\vec{r}_{\text{new}}) - u(\vec{r}_{\text{old}}))\left|\frac{\text{Det}(e^{i\vec{k}\cdot\vec{r}_{\text{new}}})}{\text{Det}(e^{i\vec{k}\cdot\vec{r}_{\text{old}}})}\right|, \tag{6}$$

where $u(\vec{r})$ is the periodic pseudopotential, which is derived in Appendix A1. To carry out the calculation of the ratio between the Slater determinant of the new and the old configurations efficiently, we use the inverse updating technique developed by Ceperley *et al.*[19] We found that the number of MC steps needed for "thermalization" is of the order of 10^5 and we use the order of 2×10^6 MC steps to calculate averages of the distribution function.

The potential energy of the high LL can be expressed[18] via the pair distribution function of the LLL using the single-mode approximation discussed in Ref. 20, namely,

$$V_L = \frac{\rho}{2}\int [g(\vec{r}) - 1] V_{\text{eff}}^L(r) d^2r, \tag{7}$$

where the effective potential $V_{\text{eff}}^L(r)$ for LL L is the convolution of the effective interaction[16]

$$V(r) = e^2/\epsilon\sqrt{r^2 + \lambda^2}, \tag{8}$$

with the L-order Laguerre polynomial; namely, it is the Fourier transform of

$$\tilde{V}_{\text{eff}}^L(q) = \frac{2\pi e^2}{\epsilon q} e^{-\lambda q}[L_L(q^2/2)]^2, \tag{9}$$

In the above formula, λ is a length scale which characterizes the confinement of the electron wave function in the direction perpendicular to the heterojunction.[16]

We use the single-mode approximation to calculate the interaction energy at high LL (Eq. (7)) and we are only interested in obtaining the pair distribution function $g(\vec{r})$. The kinetic-energy advantage of the isotropic phase over the nematic phase is calculated in Appendix A2. The approach can be divided into the following steps: (i) The pair distribution function for the LLL for different anisotropic parameters α is calculated. (ii) The single-mode approximation[20] is used to calculate the interaction energies at a high LL. (iii) The kinetic energy for different anisotropic parameters is evaluated (see Appendix A2). (iv) We compare total energies of the isotropic and nematic state to determine at what LL the nematic becomes energetically favorable. (v) The optimum value of α is determined by minimizing the total energy. (vi) The HF results, which have been reported so far,[21–23] correspond to the case of $\lambda=0$. Therefore, we needed to carry out HF calculations following Refs 21–23 for the case of the interaction given by Eq. (8) for $\lambda \neq 0$. The optimum total energies of the nematic states will be compared with those of the stripe states at different values of λ for the second excited LL to determine a critical value of λ below which the nematic state maybe energetically favorable. (vii) The above

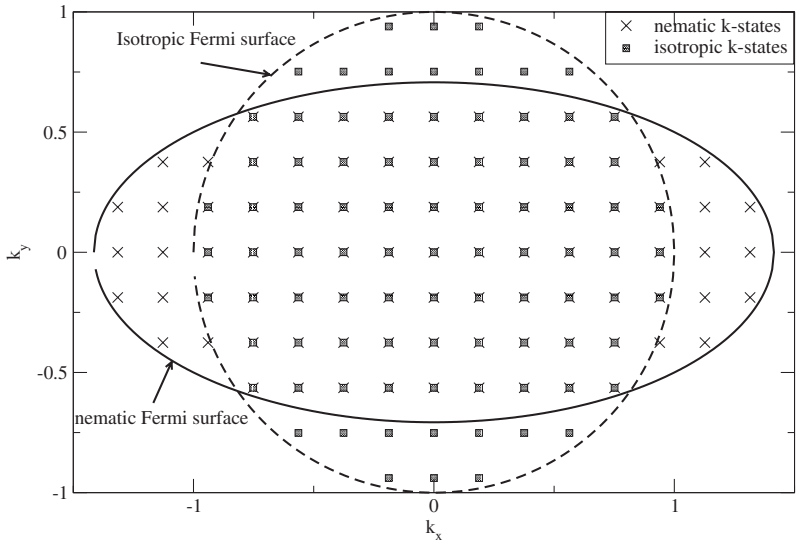

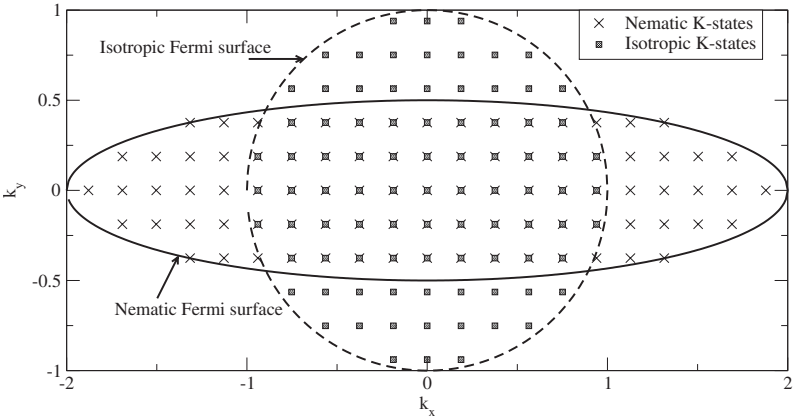

FIG. 1. Occupied states for the nematic state with $\alpha=2$ (top) and $\alpha=4$ (bottom) for the case of 89 particles.

mentioned critical value of λ is compared to the value, which corresponds to those samples used in the experiment.[1] (viii) A comparison of the MC results to the ones obtained by FHNC will also be presented.

III. RESULTS

First, we would like to note that we believe that finite-size effects are small in our MC calculation. This was concluded by comparing the potential energy and distribution function for various size lattices ranging from 89 up to 241 electrons. For example, we find that the energy is the same within statistical error bars for systems of 121 and 241 particles. In addition, we find that the critical value of λ, below which the nematic state becomes energetically favorable, remains the same (again within our statistical error bars) for the range of size systems discussed above.

The pair distribution function $g(r)$ obtained using MC integration has important differences when compared to $g(r)$ obtained by FHNC (Ref. 12) as illustrated in Fig. 2. Thus, it is important to obtain the energies of the nematic state at high LL by MC and to compare them with those obtained by FHNC.

We first compare the interaction energies obtained for different values of $\alpha>1$ with the potential energy of the isotropic state ($\alpha=1$) (Figs. 3 and 4). Notice from Figs. 3 and 4 that the potential energy of the isotropic state is lower than the potential energy of the nematic state for the first excited LL and LLL for all values of the parameter λ. The potential energy is calculated with the pseudopotential obtained using the Ewald sum as discussed in Appendix A1. Essentially the same result is also found with a pseudopotential obtained

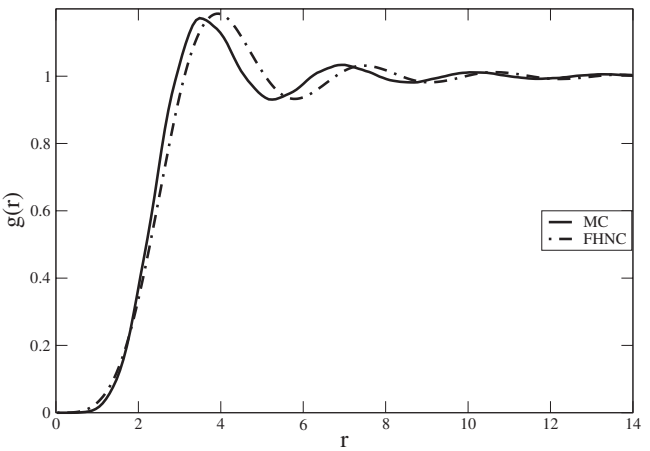

FIG. 2. Comparison of the pair distribution function obtained by FHNC and MC.

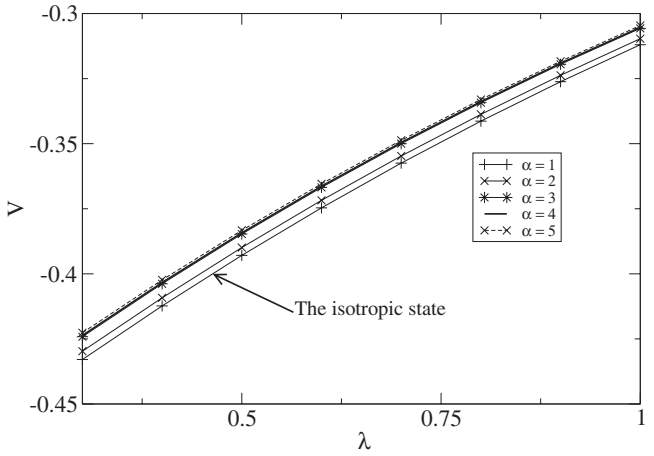

FIG. 3. Comparison of the potential energy of the nematic state calculated for various values of $\alpha \neq 1$ as function of λ with the isotropic state ($\alpha=1$) for LLL.

using the Lekner summation technique.[24] Furthermore, as shown in Appendix A2, the kinetic energy of the isotropic state is below that of the nematic state and, thus, the total energy of the isotropic state is always lower than that of the nematic state. Hence, our MC calculation shows that the isotropic state is energetically favorable as compared to the nematic state for the LLL and the first excited LL for all values of the parameter λ. Also note that the same conclusion was reached using the FHNC technique[12] with the same wave function. These findings solidify the conclusion that for the LLL and the first excited LL, the isotropic state is more stable than the nematic state, which is also in agreement with the experimental findings of Refs. 1 and 2.

For the second excited LL, however, the situation changes as illustrated in Fig. 5. The conclusion, which can be drawn from the comparison of Fig. 5, is that the interaction energy of the nematic state is lower than that of the isotropic state for all values of λ. However, we need to compare the total energy of the nematic state with that of the isotropic state for the second excited LL (Fig. 6). From Fig. 6, we conclude that the nematic state is energetically favorable as compared to

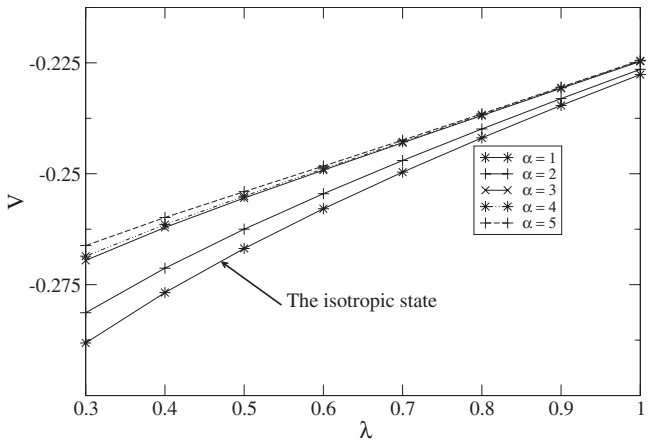

FIG. 4. Comparison of the potential energy of the nematic state calculated for various values of $\alpha \neq 1$ as function of λ with the isotropic state ($\alpha=1$) for the first excited LL.

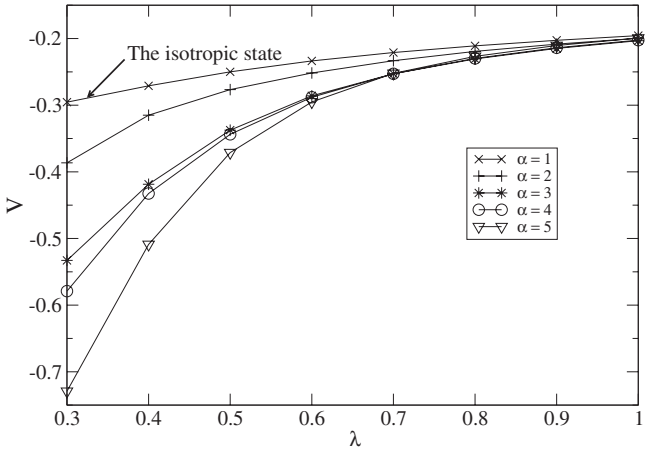

FIG. 5. Comparison between the potential energy of the nematic state calculated for various values of the anisotropic parameter $\alpha \neq 1$ as a function of λ and the potential energy of the isotropic state ($\alpha=1$) at the second excited LL.

the isotropic state for the second excited LL for the range of the parameter $\lambda \leq 0.4$. Note that in using FHNC we found[12] that for $\lambda \leq 0.6$, the total energy of the nematic state is lower than the energy of the isotropic state. In summary, both FHNC and MC yield similar conclusions about the stability of the nematic state against the isotropic state for the second excited LL.

In Refs. 3–5 the stripe-ordered phase was predicted based on HF calculations and this ordering can also explain the anisotropy observed in the transport properties of the 2DEG at low temperature. Therefore, we need to investigate the stability of the nematic state against the stripe-ordered state as follows. First, we find the optimum energies of the nematic state with respect to the anisotropic parameter α for various values of λ. Next, we compare these with the optimum energies of the stripe state obtained by the HF approximation.[21–23] Calculations for the case where $\lambda=0$ have been carried out in Refs. 21–23. For making a comparison with the optimum energy of the nematic state at various values of λ, we carried out detailed HF calculations for the

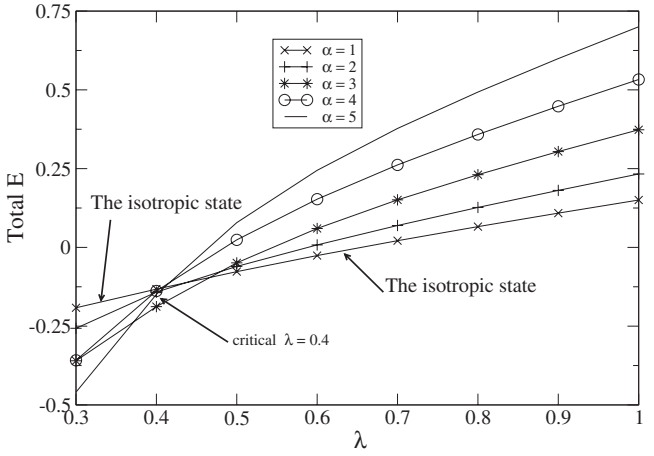

FIG. 6. Comparison of total energy of the nematic state calculated for various values of the anisotropic parameter $\alpha \neq 1$ as functions of λ with the isotropic state ($\alpha=1$) at the second excited LL.

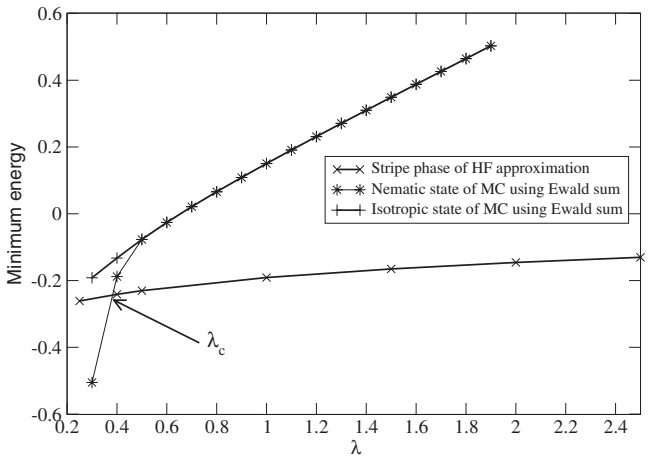

FIG. 7. Comparison of the optimal energy of the nematic state calculated by MC using the pseudopotential obtained from the Ewald sum with the stripe state calculated by HF as function of λ.

case where $\lambda \neq 0$. For the stripe-ordered state, the optimum energy is obtained by minimizing the energy with respect to the uniaxial anisotropy parameter ε defined in Ref. 23. Figure 7 shows the comparison of the optimal energies obtained by MC for the nematic state with the optimum (with respect to ε) energy for the stripe state obtained by HF. Note that for $\lambda \geq 0.5$, the optimum nematic state is obtained for $\alpha=1$, i.e., it is the isotropic state. Furthermore, Fig. 7 demonstrates that the nematic state is energetically lower than the stripe state for the values of $\lambda \leq \lambda_c = 0.37$.

In Fig. 8 we would like to present information on how large the nematicity (as measured by the parameter α) becomes for various values of the parameter λ. Figure 8(a) presents the total energy as a function of α for fixed values of the parameter λ. Notice that for $\lambda \geq 0.5$ the miminum of the total energy is achieved for $\alpha=1$, which corresponds to the isotropic case. For $\lambda=0.3$ the minimum total energy is obtained for $\alpha \sim 6.5$. In Fig. 8(b) we show this dependence of the optimum value of α as a function of λ. Notice that as λ becomes smaller and smaller the ground state quickly becomes more and more anisotropic.

As discussed earlier, the pseudopotential can be obtained by using either the Ewald or the Lekner summation technique.[24] We have also carried out the same calculation using the Lekner summation technique and the results obtained are in good agreement with those obtained using the Ewald summation method. Thus, we can conclude that with MC calculation (for $\lambda \leq \lambda_c = 0.37$), the energy of the nematic state is lower than the stripe-ordered state.

IV. CONCLUSIONS

In Fig. 9 the results for the optimum total energy of the nematic state obtained with the variational MC method is compared with that obtained by FHNC in Ref. 12 and with the optimum energy of the stripe-ordered state. The critical value of λ_c that we found from FHNC (Ref. 12) is 0.4, which is close to the value of 0.37 obtained above by MC. The critical value of λ corresponding to the sample used in the

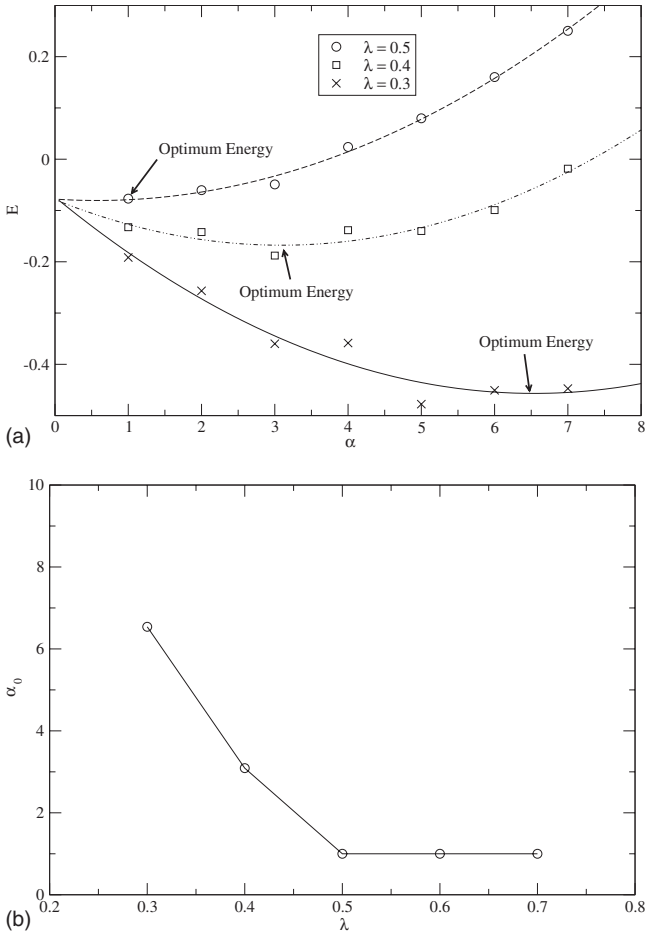

FIG. 8. (a) The total energy of the nematic state as a function of the anisotropy parameter α for various values of λ. This graph gives information on the dependence of the energy on the nematicity parameter α. (b) The optimum value of α_0 is plotted as a function of λ.

experiment,[1] which was calculated in Ref. 12—using the conditions of the experiment and sample characteristics—is approximately 0.34, which can be below the critical value found above. Thus, both MC and FHNC calculations indicate

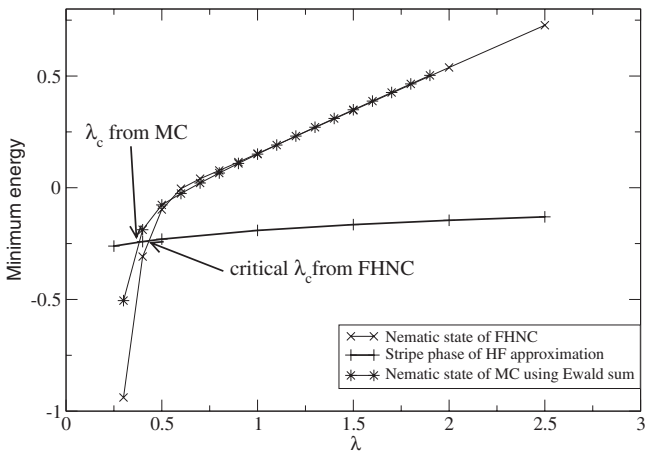

FIG. 9. Comparison of the optimum nematic state obtained from FHNC and MC with the stripe state obtained from HF.

that the nematic state might be the state observed experimentally for the 2DEG at the heterojunction in the samples used in the experiment as described in Ref. 1. There is still a remaining question about the validity of our approximation to neglect the projection operator in the wave function [Eq. (1)]. However, in both FHNC treatments of the problem,[12,18] where—in addition to neglecting the projection operator for arguments presented there—there was a second rather annoying question (yet rather straightforward to answer) of the validity of the FHNC approximation in evaluating the energy expectation value. In the present paper, the latter question is answered by employing the MC method. Therefore, we conclude that the present calculations eliminate the suspicion that the conclusions drawn in Ref. 12 might be due to an artifact of the FHNC approximation employed in Ref. 12.

ACKNOWLEDGMENTS

We would like to thank Eduardo Fradkin, Steve Kivelson, and Kun Yang and Lloyd Engel for their useful discussions.

APPENDIX

1. Ewald summation technique for the logarithmic potential

The long-range nature of the pseudopotential $\ln(r)$, which appears in the exponent of the wave function of the Jastrow factor in the case of periodic boundary conditions, requires a summation over all periodic image charges. Specifically, the "charge" distribution required to give rise to a logarithmic interaction is given as

$$\rho(\vec{r}) = \sum_{\vec{R}} \delta(\vec{r} - \vec{R}) + \rho_{\text{background}}. \tag{A1}$$

The 2D Poisson equation is given by

$$\nabla^2 \Phi(\vec{r}) = -2\pi\rho(\vec{r}), \tag{A2}$$

and its solution in 2D is the logarithmic interaction. We need to solve the above equation for a periodic square $L \times L$. The idea of Ewald summation is to add around each charge an opposite Gaussian charge distribution of an appropriately chosen width μ and, in addition, to subtract the same Gaussian charge distribution. Let us split ρ into long-range and short-range portions in the following manner:

$$\rho(\vec{r}) = \rho_1(\vec{r}) + \rho_2(\vec{r}), \tag{A3}$$

$$\rho_1(\vec{r}) = \sum_{\vec{R}} \frac{e^{-(\vec{r}-\vec{R})^2/\mu^2}}{\pi\mu^2} + \rho_{\text{background}}, \tag{A4}$$

$$\rho_2(\vec{r}) = \sum_{\vec{R}} \left[\delta(\vec{r} - \vec{R}) - \frac{e^{-(\vec{r}-\vec{R})^2/\mu^2}}{\pi\mu^2} \right], \tag{A5}$$

ϕ_1, which corresponds to ρ_1, is a short-range potential and, thus, we can calculate ϕ_1 in real space since it converges very quickly. The other combined charge configuration, i.e., ρ_2, consisting of the Gaussian and the background charge and the corresponding potential is denoted by ϕ_2. Since ϕ_2 is a long-range potential, it will be calculated in Fourier space. The solution to each of the Poisson's equations for the two charge distributions and the corresponding potential is straightforward. We note that for our case the "charge" of the particle is $e^2 = 2m$. We find

$$\phi_1(\vec{r}) = \frac{4m\pi}{A} \sum_{\vec{k}\neq 0} \frac{e^{-\mu^2 k^2/4}}{k^2} e^{i\vec{k}\cdot\vec{r}}, \tag{A6}$$

$$\phi_2(\vec{r}) = -m \sum_{\vec{R}} Ei\left[-\frac{(\vec{r}-\vec{R})^2}{\mu^2} \right]. \tag{A7}$$

where $\vec{k} = 2\pi/L\vec{n}$ with $\vec{n} \in Z^2$ and $Ei(t)$ is the exponential integral function and is defined by $Ei(t) = -\int_{-t}^{\infty} \frac{e^{-x}}{x} dx$.

For the Ewald summation, the convergence of Eqs. (A6) and (A7) is achieved choosing the width of the Gaussian charge distribution $\mu = 1$, the number of cells for the sum in Eq. (A7) to be 10 and by carrying out the sum in momentum space in Eq. (A6) over 200 k states.

In order to check the validity of this approach for the case of our use of toroidal boundary conditions, we calculated the distribution function and the energy for the 1/3 ($m=3$) case using the expressions (A6) and (A7) and our results for the energy and distribution function are identical to the results of Morf and Halperin,[25] who used the disk geometry.

2. Evaluation of kinetic energy of the nematic state

In this section of the appendix, we compute the kinetic-energy difference between the nematic and the isotropic states. In the single-LL approximation, the kinetic energy is quenched. In addition, the same is true in the HF treatment of the stripe, namely, there is no kinetic energy due to any correlation factors or operators. While this approximation gives a significant difference between the potential energy of the isotropic and the nematic states, it gives no difference between their kinetic energies, which is unacceptable because of the difference in the geometry of the Fermi sea. We want to estimate this difference. We can start with

$$(\vec{\nabla} - \vec{A})^2 F\Phi, \tag{A8}$$

$$= (\vec{\nabla} - \vec{A})^2 F\Phi + 2[(\vec{\nabla} - \vec{A})F]\nabla\Phi + F\nabla^2\Phi. \tag{A9}$$

The first term in the above equation yields

$$(\vec{\nabla} - \vec{A})^2 F\Phi = \frac{\hbar\omega_c}{2} F\Phi, \tag{A10}$$

which is common for all states under our consideration, so for simplicity we can drop it. The last term is

$$F\nabla^2\Phi = F\sum_k \frac{\hbar^2 k^2}{2m^\star}\Phi. \tag{A11}$$

So the contribution of the last term is

$$\sum_{\vec{k}\in FFS} \frac{\hbar^2 k^2}{2m^\star}, \tag{A12}$$

where $\vec{k} \in FFS$ stands for a summation over all vectors $\vec{k}$ in the corresponding filled Fermi sea. The summation over the circular Fermi sea in the isotropic case is given by

$$\frac{1}{N}\sum_{\vec{k}} \frac{\hbar^2 k^2}{2m^\star} = \frac{\hbar^2 k_F^2}{4m^\star}, \tag{A13}$$

and in the case of the elliptical Fermi sea in the anisotropic case, the summation is given by

$$\frac{1}{N}\sum_{\vec{k}} \frac{\hbar^2 k^2}{2m^\star} = \frac{\hbar^2}{4m^\star}\frac{k_1^2 + k_2^2}{2}. \tag{A14}$$

Using the fact that $k_F^2 = \vec{k}_1 \cdot \vec{k}_2$ and $k_1/k_2 = \alpha$, the kinetic-energy difference between the isotropic state and the nematic state is given as follows:

$$\Delta(KE) = -\frac{\hbar^2 k_F^2}{4m^\star}\frac{(1-\alpha)^2}{2\alpha}. \tag{A15}$$

[1] M. P. Lilly, K. B. Cooper, J. P. Eisenstein, L. N. Pfeiffer, and K. W. West, Phys. Rev. Lett. **82**, 394 (1999).
[2] R. R. Du, H. Störmer, D. Tsui, L. N. Pfeiffer, and K. West, Solid State Commun. **109**, 389 (1999).
[3] A. A. Koulakov, M. M. Fogler, and B. I. Shklovskii, Phys. Rev. Lett. **76**, 499 (1996).
[4] M. M. Fogler, A. A. Koulakov, and B. I. Shklovskii, Phys. Rev. B **54**, 1853 (1996).
[5] R. Moessner and J. T. Chalker, Phys. Rev. B **54**, 5006 (1996).
[6] E. H. Rezayi, F. D. M. Haldane, and K. Yang, Phys. Rev. Lett. **83**, 1219 (1999).
[7] F. D. M. Haldane, E. H. Rezayi, and K. Yang, Phys. Rev. Lett. **85**, 5396 (2000).
[8] E. Fradkin and S. A. Kivelson, Phys. Rev. B **59**, 8065 (1999).
[9] E. Fradkin, S. A. Kivelson, E. Manousakis, and K. Nho, Phys. Rev. Lett. **84**, 1982 (2000).
[10] K. B. Cooper, M. P. Lilly, J. P. Eisenstein, L. N. Pfeiffer, and K. W. West, Phys. Rev. B **65**, 241313(R) (2002).
[11] C. Wexler and A. T. Dorsey, Phys. Rev. B **64**, 115312 (2001).
[12] Q. M. Doan and E. Manousakis, Phys. Rev. B **75**, 195433 (2007).
[13] V. Oganesyan, S. A. Kivelson, and E. Fradkin, Phys. Rev. B **64**, 195109 (2001).
[14] R. B. Laughlin, Phys. Rev. Lett. **50**, 1395 (1983).
[15] E. Rezayi and N. Read, Phys. Rev. Lett. **72**, 900 (1994).
[16] F. C. Zhang and S. DasSarma, Phys. Rev. B **33**, 2903 (1986).
[17] E. Manousakis, S. Fantoni, V. R. Pandharipande, and Q. N. Usmani, Phys. Rev. B **28**, 3770 (1983).
[18] O. Ciftja and S. Fantoni, Phys. Rev. B **58**, 7898 (1998).
[19] D. Ceperley, G. V. Chester, and M. H. Kalos, Phys. Rev. B **16**, 3081 (1977).
[20] A. H. MacDonald and S. M. Girvin, Phys. Rev. B **33**, 4009 (1986).
[21] R. Cote and A. H. MacDonald, Phys. Rev. B **44**, 8759 (1991).
[22] R. Cote, C. B. Doiron, J. Bourassa, and H. A. Fertig, Phys. Rev. B **68**, 155327 (2003).
[23] A. M. Ettouhami, C. B. Doiron, F. D. Klironomos, R. Cote, and A. T. Dorsey, Phys. Rev. Lett. **96**, 196802 (2006).
[24] N. Gronbech-Jensen, Comput. Phys. Commun. **119**, 115 (1999).
[25] R. Morf and B. I. Halperin, Phys. Rev. B **33**, 2221 (1986).